# EXERGY ANALYSIS OF A NATURAL GAS LIQUEFACTION CASCADE CYCLE

**Hugo Valença de Araújo, hugoaraujo@feq.unicamp.br**
**José Vicente Hallak d'Angelo, dangelo@feq.unicamp.br**
Department of Chemical Systems Engineering, School of Chemical Engineering, University of Campinas, Albert Einstein Av., 500, Barão Geraldo, Campinas/SP, 13083-485, Brazil

***Abstract.*** *Nowadays, natural gas is an important energy source and its consumption tends to grow. Pipelines are the most common mean of transport for natural gas. When large distances separate the producer and the consumer, risks associated to pipelines become more significant and a liquefaction process can be used to reduce natural gas volume up to 600 times, hence producing liquefied natural gas (LNG), which enables other modes of transport. This work presents an exergy analysis of a simple cascade cycle for LNG production, aiming to contribute to further elucidate its thermodynamic performance. Main locations and causes of irreversibilities occuring in the process and ways to reduce them from a base case to an optimized one were discussed. Additionally, a parameter called exergy transfer effectiveness (ETE) was applied to quantify the exergetic efficiency in all equipment of the cascade cycle. Manipulating pressures of the streams leaving compressors and valves at each subcycle of the cascade cycle, total exergy destruction rate was decreased from 18626.01 kJ/h in the base case to 9649.47 kJ/h in the optimized case. Free expansion in valves represented the most important cause of irreversibilities, accounting for about 50% of total exergy destruction rate in both base case and optimized case. Irreversibilities generation verified in heat exchangers and compressors correspond to approximately to 30% and 20% of the total, respectively, also in both base case and optimized case. Despite exergy destruction rates decrease significantly in all equipment from the base case to the optimized one, ETE increases more expressively only in heat exchangers and some valves, and very little pronounced reductions of ETE occurred only in some compressors.*

***Keywords***: *compression refrigeration, LNG, irreversibility, exergy transfer effectiveness, exergy source, exergy sink*

## 1. NOMENCLATURE

| | | | | |
|---|---|---|---|---|
| *AH* | ASPEN Hysys | – | ***Sub and superscripts*** | |
| *COP* | coefficient of performance | – | 0 | index for environmental |
| $\bar{e}^{che}$ | standard chemical exergy | kJ/kmol | C | cold |
| *ex* | specific exergy | kJ/kmol | che | chemical exergy |
| $\dot{E}x$ | exergy flow rate | kJ/h | D | destruction |
| *ETE* | exergy transfer effectiveness | – | H | hot |
| *h* | enthalpy | kJ/kmol | i | index for stream |
| $\dot{m}$ | mass flow rate | kg/h | in | inlet |
| *P* | pressure | kPa | mech | mechanical exergy |
| $\dot{Q}$ | heat load | kJ/h | out | outlet |
| *R* | gas constant | kJ/(kmol · K) | k | index for component |
| *REF* | Refprop | – | phy | physical exergy |
| *s* | entropy | kJ/(kmol · K) | ther | thermal exergy |
| *T* | temperature | K | s | surface |
| $\dot{W}$ | power | kJ/h | ***Greek symbols*** | |
| *y* | component mole fraction | – | $\gamma$ | activity coefficient |

## 2. INTRODUCTION

Nowadays, natural gas is an important energy source as a consequence of its advantages from the economic and environmental perspectives when compared to other fossil fuels. Natural gas is cleaner and can be used at low prices as fuel in vehicles or to generate power and steam in industry. Pipelines are the most common mean of transport for natural gas between producers and intermediates or end consumers. However, when large distances separate these players of the natural gas chain, risks associated to pipelines (like leakages and disruptions) become more significant and a liquefaction process can be used to reduce the natural gas volume up to 600 times, hence producing the liquefied natural gas (LNG). This liquefaction process makes possible the use of other transport options, such as ships and special trucks. For final utilization, LNG is vaporized in regasification stations.

Various LNG plants are in operation today in several countries, including one in Brazil (GásLocal plant), located in the city of Paulínia, state of São Paulo, with a production capacity of 380,000 m³ per day and responsible for supplying regions not covered by pipelines (ANP, 2010). Since the natural gas consumption tends to grow, it is expected that the role of LNG in the energy supply to the world will increase in the future. In this sense, technologies applied in natural gas processing have been studied in order to reduce their costs by means of performance improvements. Among these technologies, LNG plants are one of the main targets since they are very intensive energy consumers. In practical applications it is estimated that approximately 1181 kJ are needed to liquefy 1 kg of natural gas (Finn et al., 1999). Thus, even minor enhancements may have a great impact on fuel demand and greenhouse gases emission of a LNG facility.

Many processes are commercially available for on or offshore natural gas liquefaction and some of the most commonly used are propane pre-cooled refrigeration cycle (also known as C3MR or APCI cycle), pure-component cascade cycle, single-mixed refrigerant cycle and dual-mixed refrigerant cycle (Mokhatab et al., 2014). The general goal of all these processes is to reduce the temperature of a natural gas feed stream to about -150 °C (required for storage) and they are based on more or less complex arrangements of compression refrigeration subcycles using pure or mixture refrigerant. Typical equipment existing in LNG cycles are compressors, heat exchangers (including devices with multiple streams), valves, mixers and separators. Previous papers that have studied these cycles using different approaches include Cipolato et al. (2012), Kamalinejad et al. (2014), Kanoğlu (2002) and Yoon et al. (2012).

In view of what has been done in prior studies, the present work presents an exergy analysis of a simple cascade cycle for LNG production, aiming to contribute to further elucidate its thermodynamic performance. The exergy analysis is capable to point out locations, magnitudes and causes of inefficiencies in cycle, which are assessed in a thermodynamically consistent way since exergy considers First and Second laws of Thermodynamics at the same time (Bejan et al., 1996). Evaluation of process variables effects over irreversibilities is performed to indicate directions for cycle optimization. A similar cascade cycle configuration to the one investigated by Cipolato et al. (2012) was studied here, but new aspects not taken into account by these authors were explored. In this sense, the main causes of irreversibilities and means to reduce them from a base case to an optimized one are discussed. Additionally, a recently proposed parameter (exergy transfer effectiveness – *ETE*) was applied to quantify the efficiency of exergy transfer in all equipment of the cascade cycle.

## 3. DESCRIPTION OF NATURAL GAS LIQUEFACTION CASCADE CYCLE

A schematic of the natural gas liquefaction cascade cycle analyzed in the present work is shown in Fig. 1(a). The process is formed by three compression refrigeration subcycles coupled by means of shared heat exchangers. Pure methane, ethane and propane are the refrigerants used in the lower (streams #7 to #11), middle (#12 to #15) and upper (#16 to #19) subcycles, respectively. The main purpose is to absorb heat from the natural gas feed and finally release it to a thermal sink. To achieve this, lower subcycle extracts heat from natural gas stream in HX3 (causing a temperature decrease from stream #3 to #4) and then rejects it to middle and upper cycles at HX2 and HX1, which are multiple streams heat exchangers. In a similar way, middle subcycle extracts heat from natural gas and methane streams in HX2 (lowering the temperatures of stream #2 to #3 and of stream #8 to #9), rejecting it to upper cycle at HX1. Also note that some of heat absorption from natural gas stream occurs directly in HX1. To close the cycle, upper subcycle discharges all heat extracted from natural gas feed to a cooling water stream at HX4.

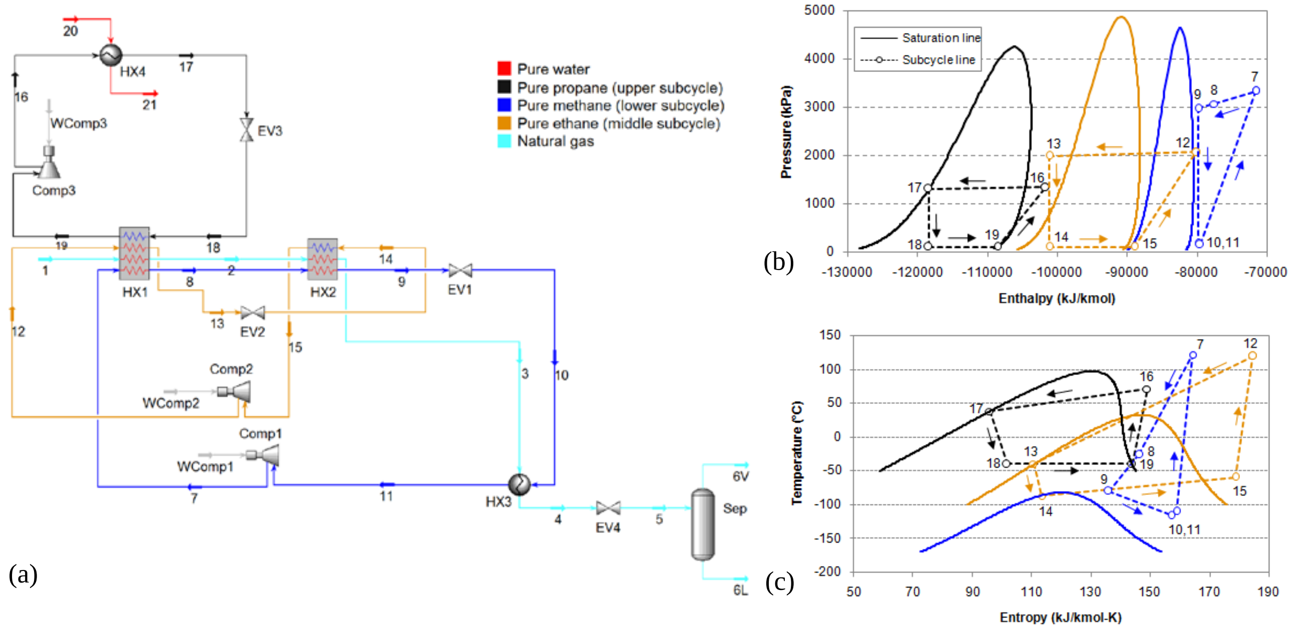

Figure 1. (a) Schematic of the cascade natural gas liquefaction cycle, (b) *P-h* diagram and (c) *T-s* diagram of subcycles (base case conditions taken from Cipolato et al., 2012).

Each one of the subcycles in Fig. 1 contains a single-stage compressor. In general, subcycles of a cascade cycle for LNG production have more than one compression stage in order to improve process efficiency and operability since power requirement can be better distributed among several compression devices. However, for the sake of simplicity of the cycle and to be possible to make some comparisons with the results from Cipolato et al. (2012), subcycles with only one compressor were considered. Particularly, in comparison to Cipolato et al. (2012), there are two differences taken into account here which are relevant: cooling water supplied to upper subcycle is available at 25 °C (stream #20) and an adiabatic flash tank (Sep) preceded by a valve (EV4) is used for separation before LNG is sent to storage. These differences were adopted in order to avoid demands for cold utilities at temperatures below the environmental temperature, which would require extra refrigeration systems.

The presence of an adiabatic flash tank instead of a flash tank releasing heat to an external sink (as considered by Cipolato et al., 2012) implies that only a percentage of total natural gas feed is obtained as liquid in conditions required for storage. In this sense, flow rate of LNG produced depends on the expansion ratio in the valve preceding the adiabatic flash tank. According to Kanoğlu (2002), storage pressures for LNG are in the range of 70–500 kPa, and temperature is -150 °C or below. Therefore, effects of storage pressure (i.e. the outlet pressure of valve preceding flash tank) on final percentage of natural gas that is liquefied and process thermodynamic performance can be evaluated. Particularly, depending on the exergy destruction rate associated to EV4 valve, its outlet pressure can be varied without great disadvantages for cycle efficiency, increasing the final fraction of LNG.

### 3.1 Operating conditions for base case and values of independent variables

Pressures of streams leaving compressors and valves of each subcycle were taken from Cipolato et al. (2012) and also represent the base case of the present work (see Fig. 1 and Tab. 1). These variables were chosen because they are easier to control in practical systems when compared to others operating variables. Remaining specifications were extracted from Filstead (1965), which presented typical values of temperature and pressure drop in several process lines. Composition of natural gas feed is also given in Tab. 1 and corresponds to that of natural gas processed at GásLocal plant (Cipolato et al., 2012). For base case conditions, *P–h* and *T–s* diagrams for pure refrigerant subcycles are shown in Figs. 1(b) and 1(c). It is observed that ethane and propane subcycles operate from one side to another of saturation curves, while all state points of methane subcycle are in superheated and supercritical regions. This happens as a consequence of values selected for process variables of methane subcycle.

For parametric analyses, variations of 10% below and above for pressure at specific points for the base case were taken into account, resulting in maximum and minimum values shown in Tab. 1. Such variations were regarded as of acceptable magnitudes and allow comprehensive investigations of trends for dependent variables. Moreover, attention must be paid to minimum temperature approaches in heat exchangers since this parameter should be maintained in such a value that a reasonable equilibrium between economic (related to equipment area) and thermodynamic performances is attained, avoiding temperature crossings.

Table 1. Base case conditions, values of independent variables and natural gas feed composition (based on Cipolato et al., 2012).

| | Pressure (kPa) | | | | |
|---|---|---|---|---|---|
| Process line | Base case | Max. value | Min. value | Natural gas composition (%mol) | |
| #7 | 3337 | 3371 | 3003 | $CH_4$ | 90.7 |
| #10 | 170 | 153 | 187 | $C_2H_6$ | 6.8 |
| #12 | 2069 | 1862 | 2276 | $C_3H_8$ | 1.3 |
| #14 | 110 | 121 | 99 | $C_4H_{10}$ | 0.3 |
| #16 | 1344 | 1210 | 1478 | $N_2$ | 0.7 |
| #18 | 110 | 121 | 99 | $O_2$ | 0.2 |

## 4. METHODOLOGY

### 4.1 Cycle simulation and properties method validation

The natural gas liquefaction cascade cycle studied in this work was simulated using simulator ASPEN Hysys V8.6 (AspenTech, 2015). Peng-Robinson-Stryjek-Vera (PRSV) equation of state was the thermodynamic model chosen to calculate properties because of its suitability to pure substances and to hydrocarbons and inorganic species mixtures. Results from ASPEN Hysys were exported to an electronic spreadsheet in which all exergy and efficiency parameters calculations were done. Codes were written in Visual Basic for Applications in order to facilitate the evaluation of effects of cycle pressures on selected thermodynamic performance metrics.

Validation of properties method was performed by comparing results of ASPEN Hysys to that from Refprop V9.1 (Lemmon et al., 2013), which is a widely used tool for calculations of thermodynamic and transport quantities for many refrigerants and mixtures. As can be seen from Figures 2(a) and 2(b), vapor pressures and specific volumes from ASPEN Hysys and Refprop are in good agreement for both pure refrigerants and natural gas mixture. Specific volume for liquid was chosen in order to verify the ability of the thermodynamic model chosen since it is an equation of state with only two adjustable parameters and originally designed to estimate quantities for gases (Klein and Nellis 2012). The highest relative deviations observed were 1.62% for vapor pressure and 7.80% for liquid specific volume. Although it is not shown, a comparison for calculated vapor specific volume also showed good agreement. Given that Refprop uses substance-specific equations of state, validation of properties method can be considered satisfactory.

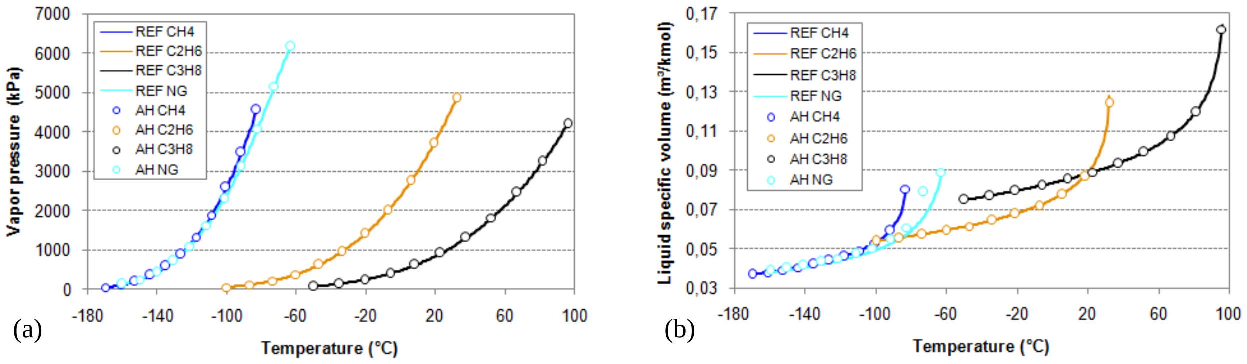

Figure 2. Comparison between (a) vapor pressures and (b) liquid specific volumes at saturation conditions for pure refrigerants and natural gas mixture (NG) from Refprop V9.1 (REF) and ASPEN Hysys V8.6 (AH).

### 4.2 Exergy analysis and thermodynamic performance metrics

Exergy is the maximum work obtainable when a system is brought from its current state to the equilibrium with a reference environment by means of reversible processes. When this equilibrium is reached, all potentials available to generate useful work are exhausted since there are no more driven forces due to temperature, pressure and chemical potential gradients. Thus, exergy provides a consistent criterion for the thermodynamic assessment of a system since all its mass and energy flow rates are measured in terms of a common basis, which is the availability to produce useful work. For this purpose, First and Second Laws of Thermodynamics are taken into account simultaneously in such a way that quantity and quality of material and energy flow rates in a system are considered (Bejan et al., 1996).

Exergy is not conserved in a system and its balance equation includes a term related to destruction, accordingly to Eq. (1), which is valid for steady-state operation. Exergy destruction rate reveals the magnitude of irreversibilities occurring in a system (Bejan et al., 1996). First and second terms at right-hand side of Eq. (1) are the inlet and outlet exergy transfer rates associated to material streams, while third and fourth ones are exergy transfer rates caused by heat and work. Neglecting kinetic and potential parts, which are usually lesser, total specific exergies of streams are determined by means of Eq. (2) as a sum of the physical and chemical contributions.

$$\dot{E}x_{\mathrm{D}} = \sum \dot{m}_{\mathrm{in}}\, ex_{\mathrm{in}} - \sum \dot{m}_{\mathrm{out}}\, ex_{\mathrm{out}} + \sum \dot{Q}_{\mathrm{s}}\left(1 - T_0/T_{\mathrm{s}}\right) - \dot{W} \tag{1}$$

$$ex_i = ex_{\mathrm{phy},\mathrm{i}} + ex_{\mathrm{che},i} \tag{2}$$

To apply Eq. (1) to an equipment of the natural gas liquefaction cascade cycle analyzed in this work, the reference environment proposed by Szargut et al. (1988) was adopted. Physical and chemical parts of total specific exergy appearing in Eq. (2) are computed by means of Eqs. (3) and (4) (Bejan et al., 1996). Temperature and pressure gradients determine physical contribution (also known as thermo-mechanical exergy) and effect of composition gradient is included in chemical contribution. For mixtures of hydrocarbons and inorganic species, activity coefficient was considered to have a weak influence on the chemical term and its value was taken as equal to unity (Rivero et al., 1999), which corresponds to the ideal solution case.

$$ex_{\mathrm{phy},\mathrm{i}} = \left(h_{\mathrm{i}} - h_{0,\mathrm{i}}\right) - T_0\left(s_{\mathrm{i}} - s_{0,i}\right) \tag{3}$$

$$ex_{\mathrm{che},i} = \sum y_{\mathrm{k,i}}\, \bar{e}_{\mathrm{i}}^{\mathrm{che}} + RT_0 \sum y_{\mathrm{k,i}} \ln\left(\gamma_{\mathrm{k,i}} \cdot y_{\mathrm{k,i}}\right) \tag{4}$$

Coefficient of performance (*COP*) was the energetic performance metric applied to evaluate natural gas cascade cycle studied in the present work. For the whole process, *COP* is computed by means of Eq. (5). *COP* is widely used for refrigeration cycles and compares the useful effect obtained to the required input (i.e. the cooling effect to the power consumed in compressors of compression refrigeration systems). Exergy efficiencies were evaluated by means of exergy transfer effectiveness (*ETE*), a parameter proposed by Marmolejo-Correa (2013) for the exergetic assessment of low temperature processes. *ETE* is defined in Eq. (6) and takes into account the concepts of exergy source and sink. Calculation of *ETE*s requires physical exergy separation into its thermal and mechanical parts, determined accordingly to Eqs. (7) and (8). For all classes of equipment existing in the cascade cycle, definitions of exergy source and sink for cases of streams above, below and across the environmental temperature are presented in Tab. 2. More details about *ETE*s and results of comparisons with other kinds of exergy efficiency are given elsewhere (Marmolejo-Correa and Gundersen 2015; Marmolejo-Correa and Gundersen 2012; Marmolejo-Correa, 2013).

$$COP = \frac{\dot{Q}_{10-11} + \dot{Q}_{14-15} + \dot{Q}_{18-19}}{\dot{W}_{\text{Comp 1}} + \dot{W}_{\text{Comp 2}} + \dot{W}_{\text{Comp 3}}} \tag{5}$$

$$ETE = \frac{\text{Exergy sink}}{\text{Exergy source}} \tag{6}$$

$$ex_{\text{ther}} = [h(T,P) - h(T_0,P)] - T_0[s(T,P) - s(T_0,P)] \tag{7}$$

$$ex_{\text{mech}} = [h(T_0,P) - h(T_0,P_0)] - T_0[s(T_0,P) - s(T_0,P_0)] \tag{8}$$

Table 2. Definitions of exergy sources and sinks for cases above, below and across $T_0$ (according to Marmolejo-Correa, 2013).

| Equipment | Stream exergy behavior | Above $T_0$ | Below $T_0$ | Across $T_0$ |
|---|---|---|---|---|
| Valve | Source | $\dot{E}x_{\text{in}}^{\text{phy}} - \dot{E}x_{\text{out}}^{\text{phy}}$ | $\dot{E}x_{\text{in}}^{\text{mech}} - \dot{E}x_{\text{out}}^{\text{mech}}$ | $\dot{E}x_{\text{in}}^{\text{mech}} - \dot{E}x_{\text{out}}^{\text{mech}} + \dot{E}x_{\text{in}}^{\text{ther}}$ |
| | Sink | Dissipative losses | $\dot{E}x_{\text{out}}^{\text{ther}} - \dot{E}x_{\text{in}}^{\text{ther}}$ | $\dot{E}x_{\text{out}}^{\text{ther}}$ |
| Compressor | Source | $\dot{W}$ | $\dot{E}x_{\text{in}}^{\text{ther}} - \dot{E}x_{\text{out}}^{\text{ther}} + \dot{W}$ | $\dot{W} + \dot{E}x_{\text{in}}^{\text{ther}}$ |
| | Sink | $\dot{E}x_{\text{out}}^{\text{phy}} - \dot{E}x_{\text{in}}^{\text{phy}}$ | $\dot{E}x_{\text{in}}^{\text{mech}} - \dot{E}x_{\text{out}}^{\text{mech}}$ | $\dot{E}x_{\text{out}}^{\text{mech}} - \dot{E}x_{\text{in}}^{\text{mech}} + \dot{E}x_{\text{out}}^{\text{ther}}$ |
| Heat exchanger | Source | $(\dot{E}x_{\text{H,in}}^{\text{ther}} - \dot{E}x_{\text{H,out}}^{\text{ther}})$<br>$+ (\dot{E}x_{\text{H,in}}^{\text{mech}} - \dot{E}x_{\text{H,out}}^{\text{mech}})$ | $(\dot{E}x_{\text{C,in}}^{\text{ther}} - \dot{E}x_{\text{C,out}}^{\text{ther}})$<br>$+ (\dot{E}x_{\text{C,in}}^{\text{mech}} - \dot{E}x_{\text{C,out}}^{\text{mech}})$ | $(\dot{E}x_{\text{C,in}}^{\text{ther}} + \dot{E}x_{\text{H,in}}^{\text{ther}})$<br>$+(\dot{E}x_{\text{H,in}}^{\text{mech}} - \dot{E}x_{\text{H},T_0}^{\text{mech}}$<br>$+\dot{E}x_{\text{C,in}}^{\text{mech}} - \dot{E}x_{\text{C},T_0}^{\text{mech}})$ |
| | Sink | $(\dot{E}x_{\text{C,out}}^{\text{ther}} - \dot{E}x_{\text{C,in}}^{\text{ther}})$<br>$- (\dot{E}x_{\text{C,in}}^{\text{mech}} - \dot{E}x_{\text{C,out}}^{\text{mech}})$ | $(\dot{E}x_{\text{H,out}}^{\text{ther}} - \dot{E}x_{\text{H,in}}^{\text{ther}})$<br>$- (\dot{E}x_{\text{H,in}}^{\text{mech}} - \dot{E}x_{\text{H,out}}^{\text{mech}})$ | $(\dot{E}x_{\text{C,out}}^{\text{ther}} + \dot{E}x_{\text{H,out}}^{\text{ther}})$<br>$-(\dot{E}x_{\text{C},T_0}^{\text{mech}} - \dot{E}x_{\text{C,out}}^{\text{mech}}$<br>$+\dot{E}x_{\text{H},T_0}^{\text{mech}} - \dot{E}x_{\text{H,out}}^{\text{mech}})$ |

## 5. RESULTS AND DISCUSSION

### 5.1 Base case analysis

For the cascade cycle at base case conditions, Figs. 3(a) and 3(b) show exergy destruction rates in each equipment and their respective percentages. It is verified that the highest exergy destruction rates occur in EV1, HX1, EV3 and Comp3. Therefore, free expansion in valves of lower and upper subcycles represents the most important cause of irreversibilities, accounting for 48% of total exergy destruction rate. Irreversibilities generation in a valve (modeled as isenthalpic) depends on the entropy increase and the material flow rate through it. Expansion ratios in valves EV2 and EV4 are greater than those in EV1 and EV3; however, due to heat loads demanded in each subcycle and refrigerants properties (like specific heat capacity, specific volume and pressure, which determines enthalpy and entropy, see Klein and Nellis, 2012), material flow rates in valves EV2 and EV4 are one and three orders of magnitude smaller in comparison to those in EV1 and EV3, respectively. Also because of some of the aforementioned reasons, entropy increase in EV2, EV3 and EV4 are relatively close, with a maximum difference of 4.13 kJ/(kmol · K), corroborating that EV3 is the most irreversible among these valves. Furthermore, Sep is a flash tank serving as a simple separator for liquid and vapor phases resulting from expansion in EV4. Therefore, no temperature, pressure and global composition variations are observed in Sep, and it does not generate irreversibilities.

Note that valve EV1 is in lower subcycle, which uses methane as refrigerant and operates in both superheated and supercritical regions, as shown in Figs. 1(b) and 1(c). This valve is associated to the greatest entropy raise, which is one order of magnitude higher than those observed in other valves, and a high material flow rate, indicating that the adoption of new values for process variables of methane subcycle can be really interesting to improve its efficiency, especially because Comp1 also generates irreversibilities in a large extent. Valve EV3 is in upper subcycle, in which the evaporation of propane is responsible for removing a great heat load from multiple streams that need to be cooled in heat exchanger HX1, implying the highest refrigerant material flow rate required. Valve EV4 brings natural gas stream to the storage conditions through the largest pressure ratio in cascade cycle, while the material flow rate of natural gas stream is the lowest one.

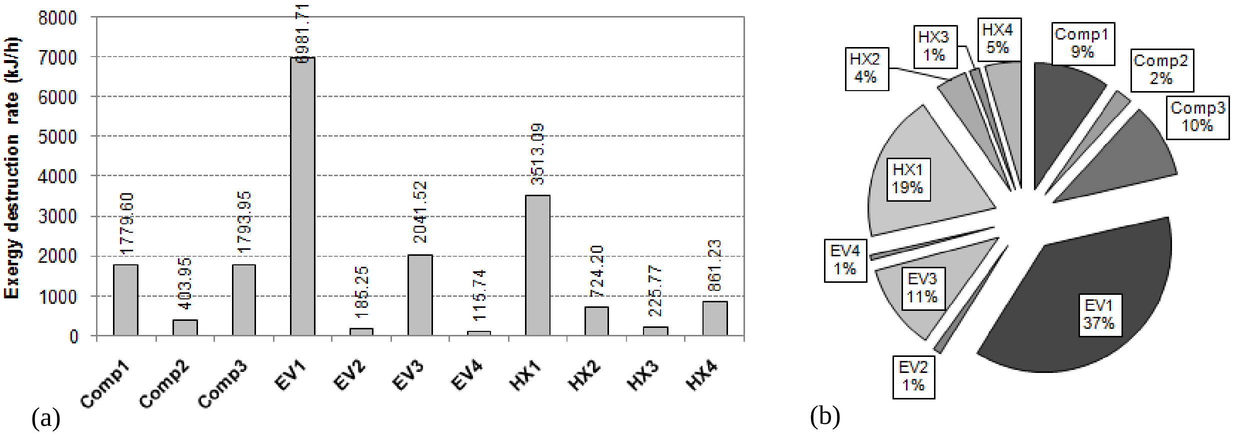

(a) (b)

Figure 3. Results for cycle at base case: (a) exergy destruction rates in equipment and (b) percentages of exergy destruction rates in equipment.

In order to decrease exergy destruction rates in valves, turbines can be used to replace them in order to produce power from the expansion process. However, this option is sometimes not feasible or economic and even more because the stream subjected to expansion is liquid, which would require advanced turbines capable to deal with it (Kanoğlu, 2001). Despite this, non-conventional power devices, like cryogenic turbines and liquid expanders, have been considered for the substitution of throttling valves in cycles for LNG production (Kanoğlu 2001; Marmolejo-Correa 2013). In this sense, Çengel and Kimmel (1997) demonstrated that a high investment cost demanded by a cryogenic turbine can be counterbalanced by an expressive saving in electricity. Moreover, another way to make generation of irreversibilities in valves less pronounced is to manipulate inlet and outlet pressures aiming to reduce the expansion ratio when it is possible for the system under consideration.

It is interesting to discuss differences amongst valves from the point of view of formation of their exergy destruction rates. Valves EV1, EV2 and EV4 operate below the environmental temperature, while the stream through EV3 crosses this temperature (i.e. enters below $T_0$ and leaves above $T_0$). Thus, although irreversibilities in valves are computed by means of direct application of exergy balances, exergetic performances of expansion devices depend on the ranges in which streams along them are exergy sources or sinks. This idea was further explored in Marmolejo-Correa and Gundersen (2015), Marmolejo-Correa and Gundersen (2012) and Marmolejo-Correa (2013), and also applies to other equipment. For valves operating entirely below environmental temperature, decrease in mechanical exergy and increase in thermal exergy are the exergy source and sink, respectively. On the other side, for valves working across the environmental temperature, variation in thermal exergy above this temperature is positive and serves as exergy source together with variation in mechanical exergy.

Figures 4(a) and 4(b) show mechanical and thermal exergies of streams in all valves and *ETE*s of these expansion devices. From Fig. 5(b), it is evident that the most inefficient valve from the thermodynamic perspective is EV1, which is the only one without refrigerant condensation, see Figs. 1(b) and 1(c), and the second one is EV3. These trends are compatible with those revealed in Fig. 4(a) because EV1 and EV3 are also the valves associated to the greatest exergy destruction rates. Although generation of irreversibilities in EV2 is a little bit more expressive, this valve presents a higher *ETE* in comparison to that of EV4, which is a consequence of a greater relative variation in thermal exergy of stream along EV2. Therefore, EV4 is more irreversible than EV2, but its *ETE* indicates that transfer from exergy source to sink is more efficient at about 14%.

Heat exchangers account for a significant share of irreversibilities generation, corresponding to 29% of total. The greatest exergy destruction rate amongst heat exchangers is observed in HX1, which is a multiple streams device, and is due to heat transfer under finite temperature differences and pressure drops. HX1 serves as a condenser for the middle subcycle stream and as a cooler for the lower subcycle and the natural gas streams, and all of them reject heat to evaporating propane. Also concerning to HX1, it is important to highlight that both methane and ethane streams release heat while crossing the environmental temperature. Consequently, methane and ethane streams can behave as exergy sources or sinks throughout HX1 depending on temperature ranges (Marmolejo-Correa, 2013). All other heat exchangers of the cascade cycle operate totally above or below the environmental temperature, so that streams through them do not change from exergy source to sink during heat exchange.

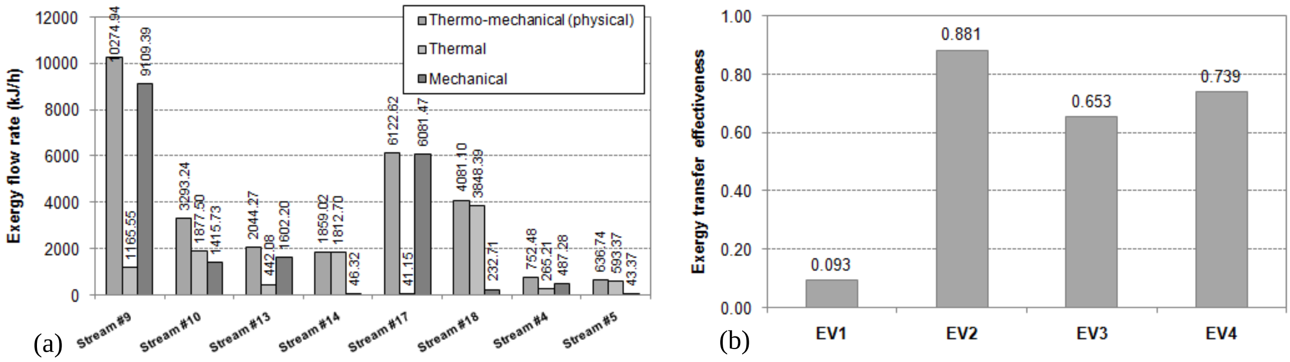

Figure 4. (a) Physical, thermal and mechanical exergies of streams through valves and (b) *ETE*s of valves.

*ETE*s of all heat exchangers in the cascade cycle are presented in Fig. 5. Formulations used to calculate these *ETE*s were defined from considerations explained in Marmolejo-Correa (2013), including exergy transfers resulting from pressure drops, whose profiles were generated assuming that d$P$/d$h$ is constant. As can be seen from Fig. 5, the most inefficient heat exchangers from the thermodynamic perspective are HX1 and HX4, in this order. According to Fig. 3(a), these heat exchangers are also the ones associated to the highest exergy destruction rates. Additionally, despite HX2 generates more irreversibilities than HX3, see Fig. 3(a), transfer from exergy source to sink is more efficient at about 20% in HX2. Reason for this can be assigned to the prevailing effect of exergy sink in HX2 due to two hot streams completely below environmental temperature passing through this device, while only one hot stream pass through HX3.

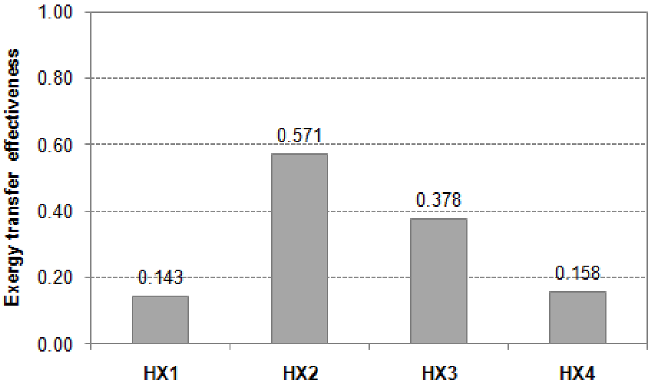

Figure 5. *ETE*s of heat exchangers.

Compression is the operation associated to the lowest exergy destruction rate in the cascade cycle, equivalent to 21% of total, but it is still relevant and can be improved. It was assumed that all compressors work under the same isentropic efficiency, which was fixed at a typical value of 0.75. Analogously to a valve, exergy destruction rate in a compressor is determined by the entropy increase and the material flow rate along it. Compressor of middle subcycle (i.e. Comp2) is the less irreversible due to the same reason already assigned to low generation of irreversibilities in the valve of this subcycle. Between Comp1 and Comp3, the first one is a little bit less irreversible despite of the higher material flow rate through it, which is counterbalanced by a great entropy raise due to refrigerant properties under inlet and outlet conditions of Comp1.

Exergy destruction rates in compressors are caused mainly by friction and can be decreased by means of using more efficient compression devices. However, compressors with higher isentropic efficiencies are more expensive and an acceptable balance between the thermodynamic performance gain and the greater capital cost required should be attained. Another way to reduce generation of irreversibilities in a compressor is to control the compression ratio, so that this process variable can be manipulated when it is admissible to change inlet and outlet pressures. Additionally, all compressors of the cascade cycle work from below to above the environmental temperature. Just as for valves and heat exchangers, this is an important fact to be considered in order to know in details how exergy destruction rates in compressors are formed and to calculate their *ETE*s coherently.

If a compressor is working totally above the environmental temperature, the exergy source is the power consumed and the exergy sink is the consequent raise in physical exergy from inlet to outlet. On the other side, if a compressor operates crossing the environmental temperature, variation in thermal exergy above this temperature is positive and serves as exergy source together with power requirement, while the exergy sink is the remaining part of the variation in thermal exergy plus the variation in mechanical exergy (Marmolejo-Correa, 2013). Exergies of streams passing through all compressors of cascade cycle are presented in Fig. 6(a). As shown in Fig. 6(b), although Comp2 is the less irreversible among compressors, *ETE*s of all compression devices are close, meaning that their efficiencies of transfer from exergy source to sink are similar, except for a little advantage observed for Comp1, which is also the most power intensive one, see Fig. 6(a).

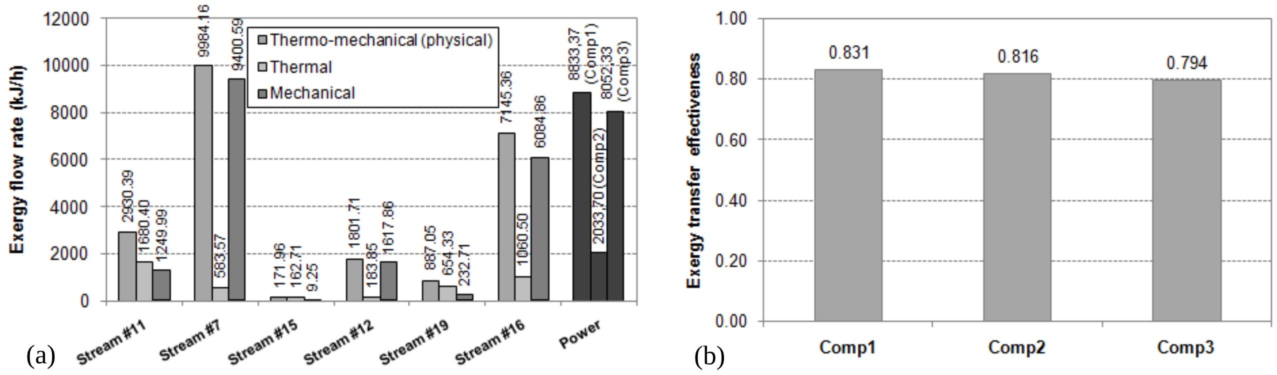

Figure 6. (a) Physical, thermal and mechanical exergies of streams through compressors, power consumed and (b) *ETE*s of compressors.

## 5.2 Optimized case analysis

Just as in Cipolato et al. (2012), 64 cases were assessed by combining minimum and maximum values of outlet pressures of valves and compressors of each subcycle, see Tab. 1. Some of these cases resulted in temperature crossing in heat exchanger HX1 and were considered not feasible. All unfeasible cases occur at the highest value of $P_{18}$, which implies a higher outlet temperature of valve EV3 and the consequent temperature crossing in HX1. For some combinations, Cipolato et al. (2012) observed temperature crossings in both HX1 and HX4; however, due to different conditions considered for cooling water (streams #20 and #21), no heat exchange inconsistency was verified in HX4 in the present work. Additionally, pressures associated to the lowest total exergy destruction rate of cascade cycle, which are given in Tab. 3, are equal to those provided in Cipolato et al. (2012) for streams #7, #10, #12 and #14, and different for streams #16 and #18 due to the temperature crossings verified by Cipolato et al. (2012), which motivated these authors to keep base case values for $P_{16}$ and $P_{18}$.

As shown in Fig. 7(a), irreversibilities generation decreases in all equipment from the base case to the optimized one, except in EV4, but inlet and outlet conditions in this valve do not change. As evidenced in Fig. 7(b), in the same way as for the base case, EV1, HX1, EV3 and Comp3 are the equipment in which the greatest exergy destruction rates are verified. Among them, in descending order, more pronounced reductions in irreversibilities are observed in EV3, Comp3, HX1 and EV1. It is important to mention that expansion and compression ratios do not vary significantly from the base case to the optimized one. In this sense, although specific irreversibilities generation in expansion and compression devices almost does not change, material flow rates through them decrease in an expressive way, as shown in Fig. 8(a), resulting in reductions of their exergy destruction rates. Total exergy destruction rate is decreased from 18626.01 kJ/h in base case to 9649.47 kJ/h in optimized case, corresponding to a reduction of almost 48%.

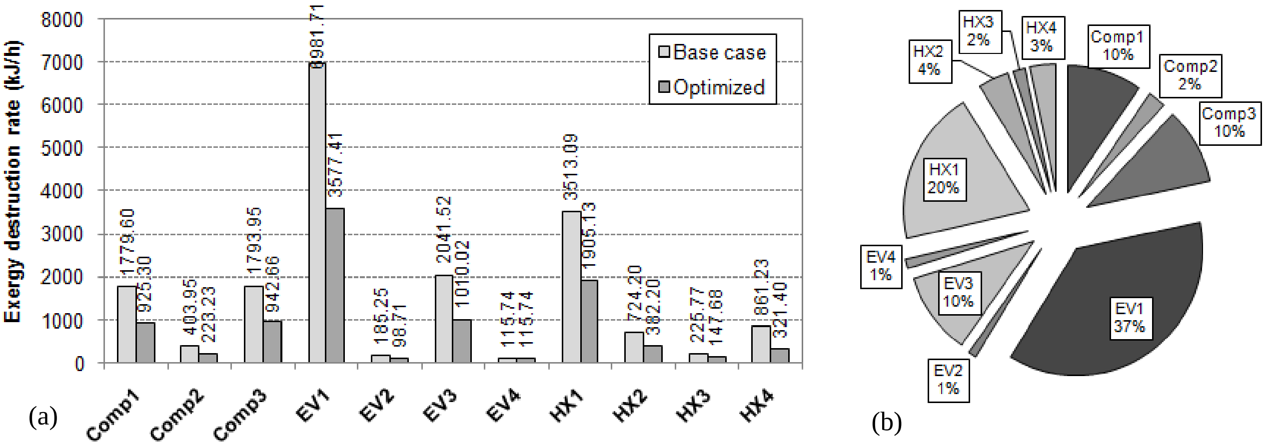

Figure 7. (a) Exergy destruction rates in equipment in base and optimized cases and (b) percentages of exergy destruction rates in equipment of optimized case.

Table 3. Pressures associated to the lowest total exergy destruction rate (optimized case).

| Pressures of process lines (kPa) | | | | | |
|---|---|---|---|---|---|
| #7 | #10 | #12 | #14 | #16 | #18 |
| 3671 | 187 | 1862 | 121 | 1210 | 99 |

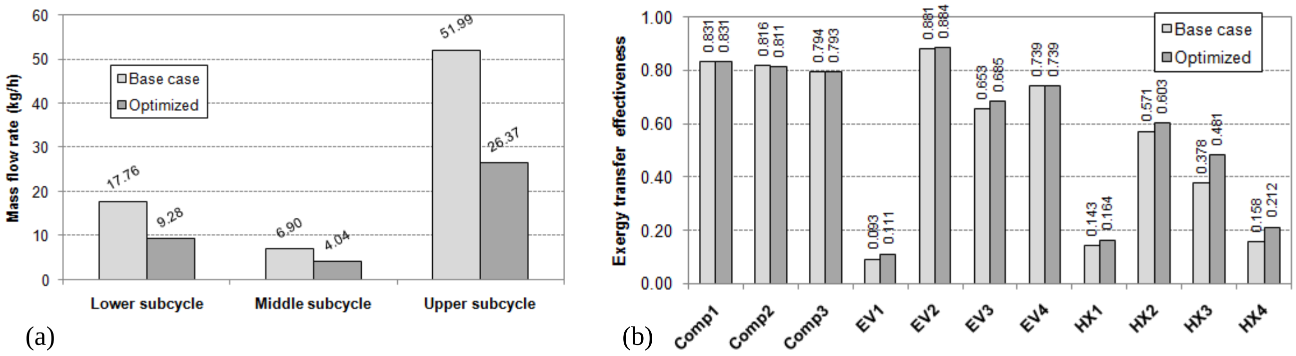

Figure 8. (a) Refrigerant flow rates in each subcycle in base and optimized cases and (b) *ETE*s of all equipment in base and optimized cases.

Reductions in material flow rates can be taken as a result of a greater specific enthalpy variation from stream #10 to #11 in methane subcycle, which is increased from 209.53 to 401.06 kJ/kmol. Since inlet and outlet conditions of natural gas stream in heat exchanger HX4 are fixed and do not change from base case to the optimized one, a smaller methane material flow rate is necessary to remove the same heat load from stream #3 and #4. Inlet and outlet conditions of natural gas stream in multiple streams heat exchangers HX1 and HX2 also do not change. Therefore, considering that ethane subcycle is removing the same heat load from stream #2 to #3 and a lower one from stream #8 to #9 due to its smaller material flow rate, a smaller flow rate of ethane is required as well. Similar reasoning applies to the propane subcycle, given that methane and ethane material flow rates are smaller, while natural gas one is the same. Specific enthalpy variations from stream #14 to #15 are almost the same in base and optimized cases, and this variation is a decrease. On the other side, specific enthalpy increase from stream #18 to #19 (9819.86 to 10293.80 kJ/kmol) is expressive and intensifies the effect of the lower heat load removal on material flow rate.

*ETE*s for all equipment in base and optimized cases are given in Fig. 8(b). Exergy behaviors of streams are the same in base and optimized cases. Despite exergy destruction rates decrease significantly in all equipment, see Fig. 7(a), Fig. 8(b) reveals that *ETE* changes more expressively only in heat exchangers and some valves, and very little pronounced reductions of *ETE* occur only in Comp2 and Comp3. Reason for this is that exergy destruction rate indicates the magnitude of irreversibilities, while exergy transfer effectiveness considers the process of irreversibilities generation by means of the exergy transfer from source to sink. In view of Eqs. (6) and (9), relation between exergy destruction rate and *ETE* is given by Eq. (10) (Marmolejo-Correa, 2013). Therefore, it is possible to affirm that decreases in exergy destruction rate counterbalancing reductions of exergy source are observed in heat exchangers and valves EV1 and EV3 in such a way that *ETE*s of these devices increase. This is also valid for heat exchangers.

$$\dot{Ex}_{\mathrm{D}} = \text{Exergy source} - \text{Exergy sink} \tag{9}$$

$$ETE = 1 - \left(\dot{Ex}_{\mathrm{D}} / \text{Exergy source}\right) \tag{10}$$

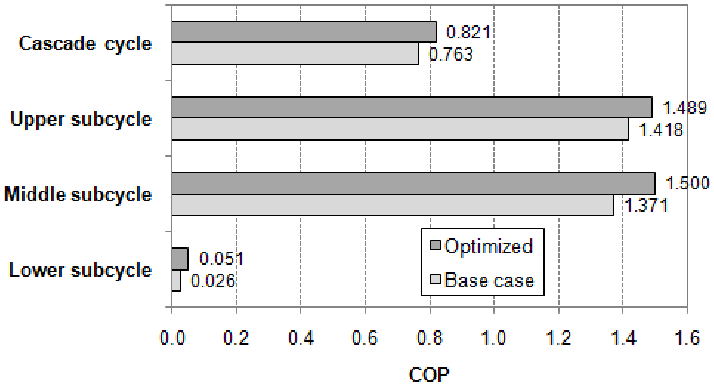

Figure 9. Values of *COP* for each subcycle and cascade cycle.

Finally, Fig. 9 shows values of *COP* for each subcycle and the entire cascade cycle. *COP* reflects variations of compression power and refrigeration load. In all subcycles, as already explained, refrigeration load decreases mainly as a consequence of smaller refrigerant flow rates, see Fig. 8(a). For compressors, specific enthalpy variations change more expressively from base to optimized case only in Comp2 (8862.28 to 8093.89 kJ/kmol), so that compression power reduction also is due mainly to smaller refrigerant flow rate. Consequently, for all subcycles and the whole process, reductions in refrigeration load and compression power from the base case to the optimized one result in increases in *COP*, as shown in Fig. 9. *COP* of lower subcycle presents the greatest relative increase, but it is still very low in comparison to *COP* of the other subcycles. Particularly, all state points of methane subcycle remain in superheated and supercritical regions even in optimized case.

## 6. CONCLUSIONS

In this work, an exergy analysis of a simple cascade cycle for LNG production was performed in order to identify locations, magnitudes and causes of irreversibilities, which were discussed for a base case and an optimized one. Concepts of exergy source and sink were applied to compute exergy transfer effectivenesses (*ETE*) of all equipment. Outlet pressures of compressors and expansion valves in each subcycle were taken as independent variables to be manipulated in order to reach the optimized case from the base one, resulting in a decrease from 18626.01 to 9649.47 kJ/h in total exergy destruction rate. Equipment where major exergy destruction rates occur are the same in both cases: EV1, HX1, EV3 and Comp3. Free expansion, heat exchange and compression account for about 50%, 30% and 20% of total, respectively, in base and optimized cases. In heat exchangers, in addition to finite temperature differences, pressure drops also contribute in a great extent to generate irreversibilities.

Despite exergy destruction rates decrease significantly in all equipment from the base case to the optimized one, *ETE* increases more expressively only in heat exchangers and valves EV1 and EV3, and very little pronounced reductions of *ETE* occurred only in compressors Comp2 and Comp3. Reason for this is that exergy destruction rate indicates the magnitude of irreversibilities, while exergy transfer effectiveness considers the process of irreversibilities generation by means of exergy transfer from source to sink. In view of relation between exergy destruction rate and *ETE*, it is possible to affirm that decreases in exergy destruction rate counterbalancing reductions of exergy source are observed in heat exchangers and valves EV1 and EV3 in such a way that *ETE*s of these devices increase from base to optimized case. In these equipment, fraction of exergy source converted into irreversibilities becomes lower.

## 7. REFERENCES

ANP, 2010. O gás natural liquefeito no Brasil: experiência da ANP na implantação dos projetos de importação de GNL. Agência Nacional do Petróleo, Gás Natural e Biocombustíveis, Rio de Janeiro.

AspenTech, 2015. Aspen HYSYS Help Section. Aspen Technology, Burlington. <https://www.aspentech.com/>

Bejan, A., Tsatsaronis, G. and Moran, M., 1996. Thermal Design and Optimization. John Wiley & Sons, New York.

Çengel, Y.A. and Kimmel, H., 1997. “Power Recovery through Thermodynamic Expansion of Liquid Methane”. In Proceedings of the American Power Conference, 59th Annual Meeting, Chicago, Illinois, United States, pp. 271–276.

Cipolato, L., Lirani, M.C.A., Costa, T.V., Fábrega, F.M., d'Angelo, J.V.H., 2012. "Exergetic Optimization of a Refrigeration Cycle for Natural Gas Liquefaction”. Computer Aided Chemical Engineering, Vol. 31, pp. 440–44.

Filstead, C. G, 1965. “Camel LNG plant: world’s largest”. Hydrocarbon Processing, Vol. 44, No. 7, pp. 135–138.

Finn, A.J., Tomlinson, H.L. and Johnson, G.L., 1999. “Gas Processing Developments: A Special Report – Developments in Natural Gas Liquefaction”. Hydrocarbon Processing, Vol. 78, No. 4, pp. 47–60.

Kamalinejad, M., Amidpour, M. and Naenian, M.M., 2014. “Optimal Synthesis of Cascade Refrigeration in Liquefied Natural Gas Cycles by Pinch-Exergy”. Journal of Oil, Gas and Petrochemical Technology, Vol. 1, No. 1, pp. 29–44.

Kanoğlu, M., 2002. “Exergy Analysis of Multistage Cascade Refrigeration Cycle Used for Natural Gas Liquefaction”. International Journal of Energy Research, Vol. 26, No. 8, pp. 763–774.

Kanoğlu, M., 2001. “Cryogenic Turbine Efficiencies”. Exergy, An International Journal, Vol. 1, No. 3, pp. 202–208.

Klein, S. and Nellis, G., 2012. Thermodynamics. Cambridge University Press, New York.

Lemmon, E.W., Huber, M.L., McLinden, M.O., 2013. NIST Standard Reference Database 23: Reference Fluid Thermodynamic and Transport Properties–REFPROP, Version 9.1. National Institute of Standards and Technology, Gaithersburg.

Marmolejo-Correa, D. and Gundersen, T., 2015. “A New Efficiency Parameter for Exergy Analysis in Low Temperature Processes”. International Journal of Exergy, Vol. 17, No. 2, pp. 135–170.

Marmolejo-Correa, D., 2013. Analysis and Design of Low Temperature Processes with Focus on LNG – Developing New Thermodynamics Based Tools and Introducing Exergy in Design Methodologies. Ph.D. thesis, Nowergian University of Science and Technology, Trondheim, Norway.

Marmolejo-Correa, D. and Gundersen, T., 2012. “A Comparison of Exergy Efficiency Definitions with Focus on Low

Temperature Processes". Energy, Vol. 44, No. 1, pp. 477–489.

Mokhatab, S., Mak, J., Valappil, J. and Wood, D.A., 2014. Handbook of Liquefied Natural Gas. Gulf Professional Publishing, New York.

Rivero, R., Rendon, C. and Monroy, L., 1999. "The Exergy of Crude Oil Mixtures and Petroleum Fractions: Calculation and Application". International Journal of Applied Thermodynamics, Vol. 2, No. 3, pp. 115–123.

Szargut, J., Moris, D.R. and Steward, F.R., 1988. Exergy Analysis of Thermal, Chemical, and Metallurgical Processes. Hemisphere Publishing, New York.

Yoon, S., Cho, H., Lim, D.H. and Kim, J.K., 2012. "Process Design and Optimization of Natural Gas Liquefaction Processes". Chemical Engineering Transactions, Vol. 29, pp. 1585–1590.

## 8. RESPONSIBILITY NOTICE

The authors are the only responsible for the printed material included in this paper.